REVIEWS

Journal of Semiconductors
(2020) 41, 041604
doi: 10.1088/1674-4926/41/4/041604

Recent progress of morphable 3D mesostructures in advanced materials

Haoran Fu[1, †], Ke Bai[2], Yonggang Huang[3], and Yihui Zhang[2, †]

[1]Institute of Flexible Electronic Technology of Tsinghua, Zhejiang, Jiaxing 314006, China

[2]Center for Mechanics and Materials and Center for Flexible Electronics Technology, AML, Department of Engineering Mechanics, Tsinghua University, Beijing 100084, China

[3]Departments of Civil and Environmental Engineering, Mechanical Engineering, and Materials Science and Engineering, Northwestern University, Evanston, IL, 60208, USA

Abstract: Soft robots complement the existing efforts of miniaturizing conventional, rigid robots, and have the potential to revolutionize areas such as military equipment and biomedical devices. This type of system can accomplish tasks in complex and time-varying environments through geometric reconfiguration induced by diverse external stimuli, such as heat, solvent, light, electric field, magnetic field, and mechanical field. Approaches to achieve reconfigurable mesostructures are essential to the design and fabrication of soft robots. Existing studies mainly focus on four key aspects: reconfiguration mechanisms, fabrication schemes, deformation control principles, and practical applications. This review presents a detailed survey of methodologies for morphable mesostructures triggered by a wide range of stimuli, with a number of impressive examples, demonstrating high degrees of deformation complexities and varied multi-functionalities. The latest progress based on the development of new materials and unique design concepts is highlighted. An outlook on the remaining challenges and open opportunities is provided.

Key words: morphable mesostructures; reconfiguration; stimuli

Citation: H R Fu, K Bai, Y G Huang, and Y H Zhang, Recent progress of morphable 3D mesostructures in advanced materials[J]. *J. Semicond.*, 2020, 41(4), 041604. http://doi.org/10.1088/1674-4926/41/4/041604

1. Introduction

The fast development of robotics and semiconductor fabrication techniques means that robots are now evolving towards miniaturization to fulfill various emerging needs in military and medical applications, such as invisible environment monitoring, and navigation through complex and confined space (e.g., vessels in human body). However, it is challenging to scale down conventional, rigid robots to millimeter and micrometer size, due to the degradation of electromagnetic motor performance and the increase of frictional losses in bearings[1]. Moreover, these rigid components in conventional robots can hardly adapt to complex and changing environments such as the human body, which constrains their further applications. To bypass these physical limits, soft robots that utilize alternative actuation strategies and flexible designs have been developed to replace some of traditional driving and controlling mechanisms[2–4]. These robots can achieve multiple functions in miniature sizes by reversible geometric deformations induced by diverse external stimuli[5, 6]. The manufacture of these soft robots has raised many technological challenges, due to the difficulties in the precise control of deformations[7], and the limitation of reconfiguration strategies[8, 9]. Considerable efforts have been made in the development of reconfiguration techniques for 3D mesostructures, ranging from reconfiguration mechanisms and fabrication schemes, to deformation control principles and unique applications.

According to different external stimuli, the reconfiguration methods can be mainly classified into six categories; that is, methods activated by thermal, chemical, optical, magnetic, electric, and mechanical fields. In this paper, we present a detailed review of methodologies for morphable mesostructures triggered by these stimuli. We also highlight the latest progress in the design concepts and applications. This review begins with an overview on the thermally activated reconfiguration method in Section 2, followed by the discussion of chemically, optically, magnetically, electrically, and mechanically responsive reconfiguration approaches in Sections 3 to 7. Finally, we provide a perspective on current challenges and opportunities for future research.

2. Methods and applications of thermally actuated reconfiguration

Thermally actuated reconfiguration approaches utilize shape-memory polymers[10–15] (SMPs), shape-memory alloys[16–18] (SMAs), transition metal oxides[19–21], liquid crystal elastomers[22–26] (LCEs) or thermally responsive hydrogel[27–30] to achieve reversible deformations. Thermally responsive morphable mesostructures can be activated remotely, either by light or thermal radiation. However, their response time is relatively slow, ranging from several seconds[31] to several minutes[32], except for transition metal oxides (hundreds of picosecond to several milliseconds[33, 34]).

Correspondence to: H R Fu, fuhaoran@ifet-tsinghua.org; Y H Zhang, yihuizhang@tsinghua.edu.cn

Received 24 OCTOBER 2019; Revised 11 DECEMBER 2019.

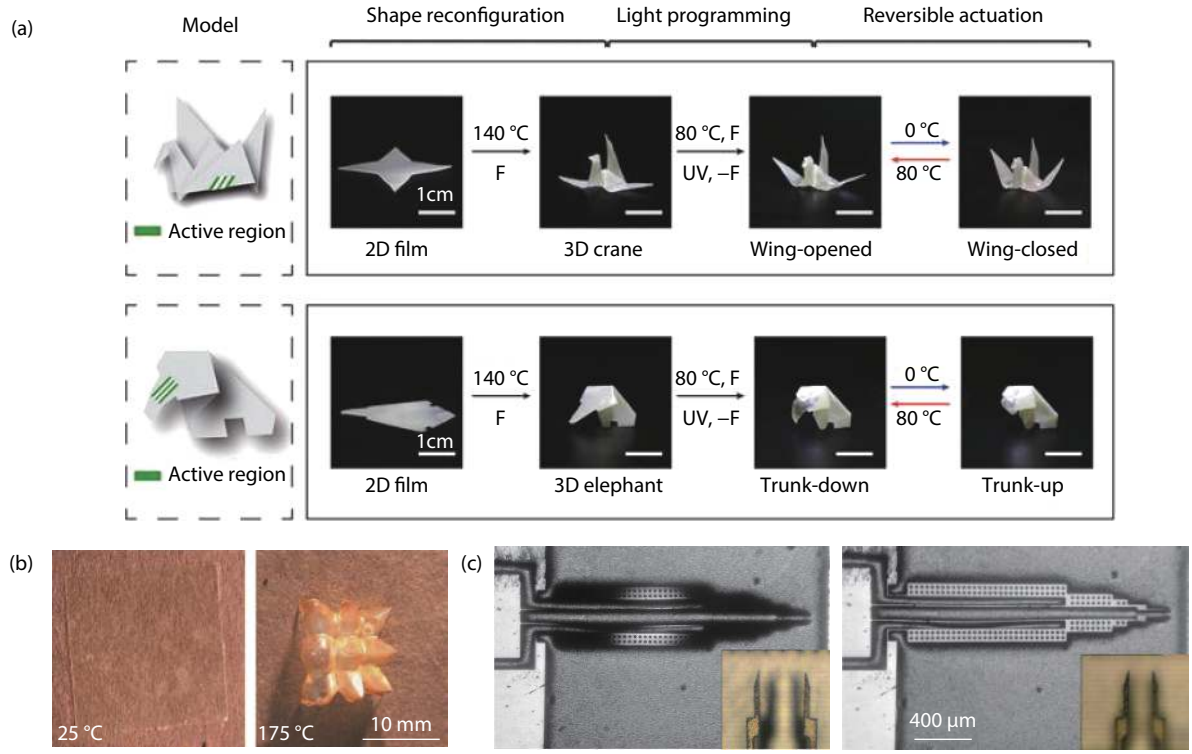

Fig. 1. (Color online) Methods and applications of thermally actuated reconfiguration. (a) Shape evolution of two morphable mesostructures made of shape-memory polymers. Reproduced with permission from Ref. [32]. Copyright 2018, AAAS. (b) Shape evolution of LCE with mesogens aligned in groups. Reproduced with permission from Ref. [22]. Copyright 2015, AAAS. (c) Demonstration of a thermally actuated micro-tweezer made of SMA. Reproduced with permission from Ref. [18]. Copyright 2007, IOP Publishing Ltd.

SMPs are one of the most commonly used active materials for thermally activated reconfiguration. In contrast to traditional SMPs, with one-way actuation governed by the glass transition temperature, reversible SMPs are determined by two temperatures: T_g, the glass transition point, and T_{low}, a lower glass transition point. After the material is deformed by an external force above T_g, it retains the temporary geometry (shape A) upon cooling to below T_{low}. When it is reheated to an intermediate temperature between T_{low} and T_g, a third configuration (shape B) occurs. Two-way SMP can be reshaped between A and B by changing the temperature, as long as the temperature remains below T_g[13]. Fig. 1(a) shows two morphable structures actuated by a combination of one-way and two-way shape-memory actuation. These 2D films were first permanently deformed into a 3D crane and a 3D elephant by thermally induced plasticity. Next, the actuation of elongation/contraction was spatio-selectively programmed into the 3D architectures (highlighted in green) by light, transforming the local region into two-way SMPs. Finally, reversible flipping movement of the wings and trunk can be triggered by temperature change[32].

Multilayers with different thermal expansion coefficients[35, 36] can also be used to enable the reconfiguration. Upon heating, the strain mismatch induces a bending moment that bends/folds the architecture into a different shape. Multilayers with different thermally responsive swelling ratios[37, 38] are similar as the thermally responsive counterpart, except for the aqueous environment. For instance, poly-(N-isopropylacrylamide) copolymer containing 1 mol% of 4-acryloylbenzophenone comonomer (poly(NIPAM–ABP)) can reversibly change its solubility in the temperature range of 10–28 °C, and polycaprolactone (PCL) is hydrophobic and water-insoluble. Fabrication of star-shape bilayer of poly (NIPAM–ABP) and PCL resulted in the formation of a gripper that can fold and unfold reversibly. Moreover, because of its partial biodegradablility, this self-folding gripper can be potentially used for encapsulation and release of cells[37].

LCEs are a kind of hybrid materials, in which polymer chains are crosslinked with oriented liquid crystal units, due to the chemical synthesis. Upon heating, mesogen chains are rearranged from anisotropic conformation to coil conformation, resulting in a reversible phase transition of the material, and accordingly, a shape change of the mesostructures[39–41]. As shown in Fig. 1(b), nine cones arise from the LCE film with an actuation of ~55% strain after heating to 175 °C[22]. In addition, exchangeable covalent bonds can replace permanent network crosslinks in LCES by transesterification, enabling the controlled alignment of liquid crystal units, thereby providing a robust method for molding the reconfigured shapes in any dimension[26]. Moreover, by dispersing carbon nanotubes into LCEs with exchangeable links, the reconfiguration process can be triggered both globally and locally, with the photothermal effects of infrared radiation at extremely low temperature (e.g., –130 °C)[24]. By incorporating LCE bilayer with orthogonal director (the direction of contractile strain) alignment and different phase transition temperatures, a self-propelled structure can be created, based on the sequential folding and unfolding in response to thermal stimuli[2]. LCEs can be further fabricated in a film or tubular shape, and incorporated with deformable resistive heaters in strategic locations, such that the bending or contracting deformations can be actuated by sequential Joule heating, suggesting applica-

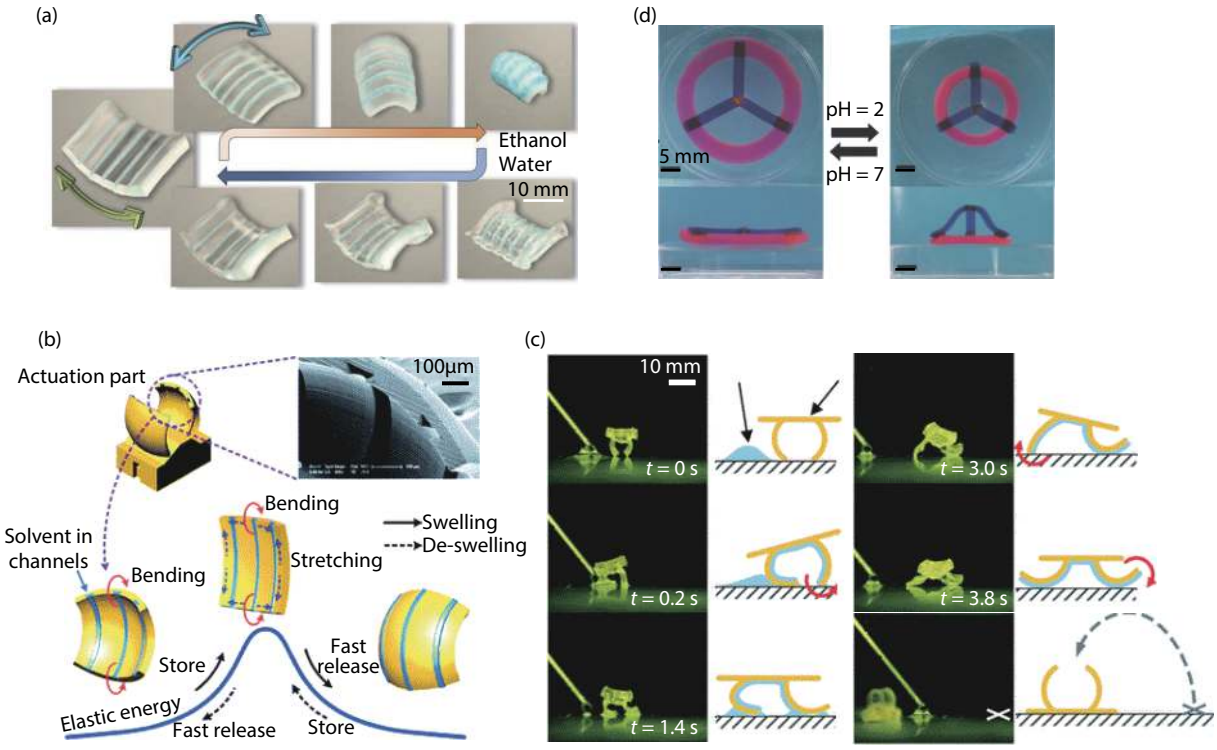

Fig. 2. (Color online) Methods and applications of chemically actuated reconfiguration. (a) Shape evolution of an ionoprinted hydrogel subject to different solvents. Reproduced with permission from Ref. [60]. Copyright 2013, Macmillan Publishers Limited. (b) Schematic illustration of a 3D jump micro hydrogel device, and scanning electron microscope (SEM) image of embedded microfluidic channels. Reproduced with permission from Ref. [61]. Copyright 2010, The Royal Society of Chemistry. (c) Evolution of the micro hydrogel device induced with a liquid solvent. Reproduced with permission from Ref. [61]. Copyright 2010, The Royal Society of Chemistry. (d) 2D-to-3D shape transformation of a tri-layer hydrogel subject to a variant pH. Reproduced with permission from Ref. [68]. Copyright 2014, John Wiley & Sons Inc.

tions in adaptive soft robots[42] and grippers[43].

Two-way SMAs are a group of metallic alloys that can experience the phase transition between martensitic and austenitic crystal structures, providing a route to the reconfiguration of their shapes or sizes. Once its temperature exceeds the austenite-start temperature, SMA begins to shrink and transform from martensite to austenite phase. When it is re-cooled below the martensite-start temperature, it can revert to martensite phase again. This transformation can produce significant strain and actuation force, with an energy density as high as 1226 J/kg[44], highlighting the potential use for micro-grippers[45], and micro flying robots[46, 47]. Fig. 1(c) shows a micro-tweezer fabricated by TiNiCu films[18]. The device consists of two arms, and each arm is made of one wide beam and one narrow beam. When subject to the Joule heating, the difference of thermal expansion in two beams leads to a horizontal actuation up to 50 μm, and the two-way shape-memory effect results in a vertical movement up to 40 μm.

Transition metal oxides represent another type of inorganic phase-change material. Among them, vanadium dioxide (VO_2) is widely used for actuators and morphable mesostructures, owing to its high work density (~7 J/cm^3)[48], which can induce large transformation strain (1%–2%)[49] through reversible insulator-metal transition (IMT) at ~68 °C. Specifically, the crystal structure of VO_2 is tetragonal in its metallic phase, and it changes to the monoclinic phase when cooled through the IMT, in which the vanadium ions are reordered and the number of unit cell doubles. Diverse rolling configurations can be fabricated by misaligning the crystal orientation and strain direction of VO_2 nanomembranes[50]. Moreover, through the Joule heating of a freestanding V-shaped Cr/VO_2 bimorph structure, torsional microactuators with both the large driving force and rotation amplitude can be achieved, highlighting potential applications in micro-robots and artificial micromuscles[19].

3. Methods and applications of chemically actuated reconfiguration

Most of the chemically actuated reconfiguration approaches rely on a liquid environment. When immersed in water, acids, organic solvents or ionic solution, soft materials (i.e., hydrogels) and inorganic materials (i.e., palladium and iron phosphate) can absorb chemicals, and then mechanical stresses arise inside the material, leading to a reversible volume expansion. The response time based on this type of approaches varies a lot, ranging from several hundred milliseconds[51] to several minutes[52, 53].

By exploiting swelling deformations, diverse morphable mesostructures can be achieved with appropriate design of hydrogel multilayers[54–59]. As shown in Fig. 2(a), by ionoprinting on hydrogel, localized Cu^{2+} ions can be dispersed in anionic hydrogels, which generates stresses around the ionoprinting regions, thereby bending the hydrogel film perpendicular to the imprinted directions (green arrow). When the structure is immersed in ethanol, the stiffer ionoprinted regions guide the asymmetric shrinking and reshaping of the gel. The structure can recover to the initial shape once placed in wa-

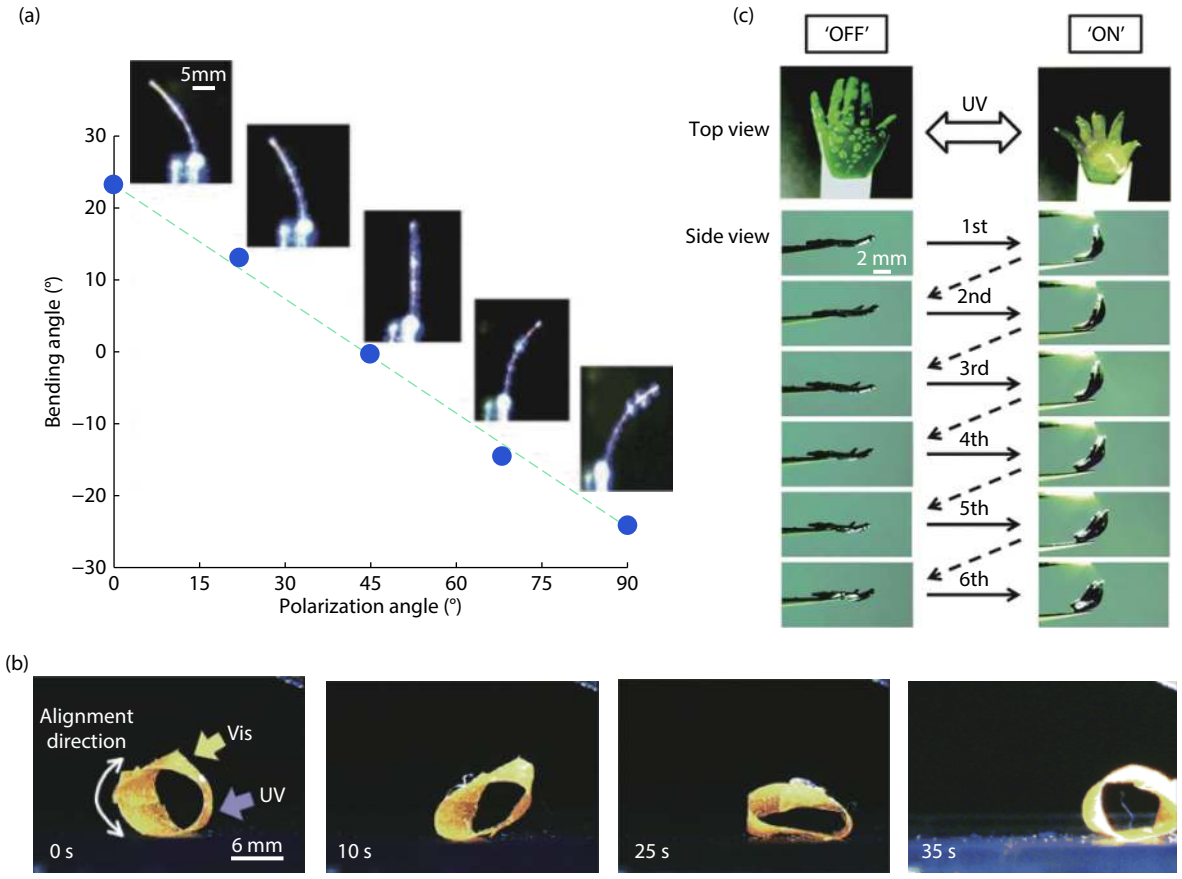

Fig. 3. (Color online) Methods and applications of optically actuated reconfiguration. (a) Bending of a cantilever made of LCE with azobenzene under the exposure of light with different polarization angles. Reproduced with permission from Ref. [80]. Copyright 2011, The Royal Society of Chemistry. (b) Rolling of a LCE film induced through the application of visible and UV light. Reproduced with permission from Ref. [82]. Copyright 2008, John Wiley & Sons Inc. (c) Shape evolution of a bilayer film with photo-initiated proton-releasing agent. Reproduced with permission from Ref. [67]. Copyright 2012, The Royal Society of Chemistry.

ter[60]. In addition, varieties of application can be accomplished, including micro robots[61] and metamaterials[62]. Figs. 2(b) and 2(c) show a micro jump robot with a high actuation speed[61]. The 3D hydrogel is fabricated by projection micro-stereo lithography, with three microfluidic channels embedded in the surface (Fig. 2(b)). The devices can change the curvature from convex to concave upon swelling, and vice versa. As shown in Fig. 2(c), when applied to the robot, the solvent droplet fills all the microfluidic networks by capillary force, resulting in the outward bending of legs. As the solvent further evaporates, the legs snap back to the original shape after the de-swelling. Similar as hydrogels, inorganic multilayers can also realize shape reconfiguration through swelling deformations. For instance, based on the reversible volume expansion of palladium (Pd) in hydrogen milieu, a microcantilever made from thin Pd/silicon bilayers can bend to different deflections with respect to the hydrogen pressure[63].Furthermore,origami-inspiredself-rolled-upnanomembranes made of titanium/chromium/Pd trilayers can reversibly transform to planar configurations after hydrogenation[64, 65], thereby decreasing the transmittance of nanomembrane arrays, which suggests potential applications in the sensitive detection of hydrogen and fabrication of high-density 3D functional devices.

Another reconfiguration approach utilizes the change of swelling ratio in multilayers when subject to a variant pH[66–68] or ionic strength[68]. Fig. 2(d) describes a shape transformation of a 2D structure made by three different hydrogels. Among these three gels, only one (red) is pH sensitive, and its swelling ratio increase as the pH rises from 3 to 7. Upon decrease of the pH, the shrinking of the red hydrogel ring pushed blue hydrogel out of plane, forming a 3D tower. This shape change is completely reversible because the 3D tower can switch back into the 2D structure without any noticeable deviation from the original shape[68]. Furthermore, this reconfiguration technique suggests potential for application in micro lens[69] and microfluidic valves[70, 71].

4. Methods and applications of optically actuated reconfiguration

Optically actuated reconfiguration approaches offer the advantage of remote control and precise activation in localized region[72]. Their response time varies from less than one millisecond[73, 74] to several minutes[75]. These approaches can be classified into two categories; that is, direct activation methods and indirect activation methods.

The direct activation methods utilize photoresponsive materials such as liquid-crystal elastomers and shape-memory polymers that are sensitive to the wavelength or polarization of the light. The photoresponsive SMPs are processed similarly with the thermally responsive SMPs, except that they are controlled by irradiation in different wavelength[76, 77]. The

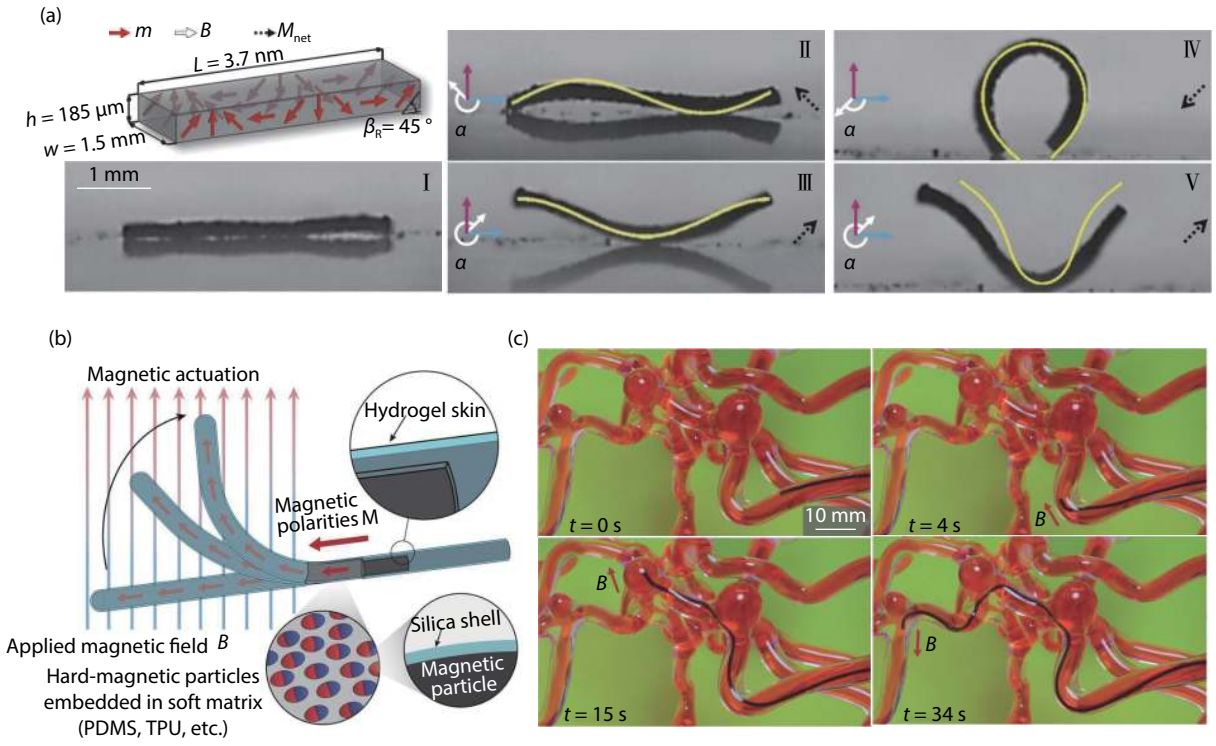

Fig. 4. (Color online) Methods and applications of magnetically actuated reconfiguration. (a) Milli-robots made of magnetoelastic soft materials. Reproduced with permission from Ref. [92]. Copyright 2018, Macmillan Publishers Limited. (b) Navigation of a ferromagnetic soft continuum robots through 3D cerebrovascular phantom network. Reproduced with permission from Ref. [96]. Copyright 2019, AAAS.

photoresponsive LCEs are fabricated using photoisomerizable molecules such as azobenzene filler. Absorption of light leads to a trans-cis isomerization of azobenzene moieties, thereby generating stresses inside the material, which substantially contracts the volume on the surface and leads to the bending of the structure[78, 79]. Fig. 3(a) shows a cantilever made of LCE with azobenzene fillers. Selective absorption of the linear polarized light allows precise control of deformation aligned with the polarization angle[80]. It can recover to the initial shape after exposure to circularly polarized light. Demonstrative applications include high frequency oscillators[73], swimming robots[81] and light driven plastic motors[82]. Fig. 3(b) depicts a photo-induced rolling motion of a continuous ring[82]. The ring is fabricated by bilayers of liquid crystal monomer and liquid crystal diacrylate with azobenzene moieties. Upon exposure to UV light (366 nm) and visible light (> 500 nm) at different regions simultaneously, the ring rolls intermittently toward the light source.

In contrast from the direct methods, the indirect activation methods exploit intermediates generated by light to reshape mesostructures. For instance, Tang *et al.* demonstrated photochemically induced actuation of liquid metal marbles[75]. The marbles are formed by encasing liquid metal galinstan (i.e., a eutectic alloy composed of 68.5% gallium, 21.5% indium, and 10% tin) with coating of WO_3 nanoparticles. When it is placed in H_2O_2 solution and illuminated with UV light, the photochemical reaction is triggered, generating oxygen bubbles that can reshape and propel the marble. Fig. 3(c) illustrates the reversible bending and straightening behavior for bilayer films made of polyacid and polybase[67]. The swelling ratio of polyacid increases first and then keeps stable with increasing the pH, while that of polybase decreases gradually with increasing the pH. When integrated with photo-initiated proton-releasing agent of o-nitrobenzaldehyde, the gel film can release proton upon UV irradiation, allowing the pH within the gel to decrease dramatically, resulting in a bent configuration. It can further straighten to the original shape when protons are diluted.

5. Methods and applications of magnetically actuated reconfiguration

Magnetically responsive morphable mesostructures are typically based on soft materials that incorporate magnetic particles[6] or individual magnets[83, 84]. When placed into an external magnetic field, the magnetic particles or individual magnets realign along the direction of magnetic field. Because the magnetic field can be tuned accurately and rapidly in terms of the magnitude and frequency, with an ability to penetrate most materials, these morphable mesostructures suggest potential use in drug delivery[85], microfluidic devices[86] and microrobots[87]. In addition, these mesostructures respond very quickly to magnetic stimuli, typically in the range of ~ 10 ms[88, 89] to 1 s[90, 91].

Generally, there are two ways to fabricate morphable mesostructures with magnetic particles. One is to load magnetic particles such as neodymium-iron-boron (NdFeB)[92] into soft compounds before casting and curing the thin polymer film. In this manner, either uniform[93] or non-uniform[6] profiles of magnetization can be generated, while the latter one need extra fabrication steps, such as exposure to external magnetic field with specific spatial distributions[88]. Fig. 4(a) presents a magnetoelastic robot with a single-wavelength harmonic magnetization *m* along its body[92]. The magnetization profile is implemented by wrapping soft robot around a cylindrical glass rod, and is then subject to a large, uniform

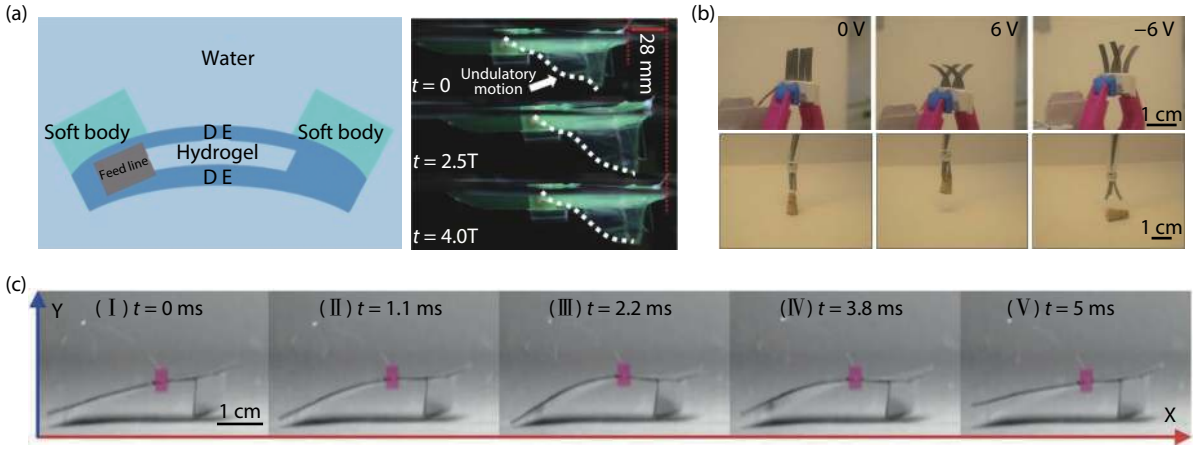

Fig. 5. (Color online) Methods and applications of electrically actuated reconfiguration. (a) Schematic illustration of a robotic fish made of DE (left-hand panel), and forward motion of the fish (right-hand panel). Reproduced with permission from Ref. [110]. Copyright 2017, AAAS. (b) Shape reconfiguration of four actuators made of IPMC (top panel), and working process of a three-finger gripper (bottom panel). Reproduced with permission from Ref. [101]. Copyright 2008, Cambridge University Press. (c) Movement of an insect-scale robot made of PVDF. Reproduced with permission from Ref. [118]. Copyright 2019, AAAS.

magnetizing field. This robot can be controlled by a time-varying magnetic field B ($B = \left[B_{xy}^T, B_z\right]^T$) to generate different modes of locomotion. The interaction between B_{xy} and m produces spatially varying magnetic torques, and hence B_{xy} can be modified to generate the desired robot configurations. Additionally, the effective magnetic moment M_{net} tends to align with B, enabling the rotation of the robot with respect to its y axis by control of B_z.

Another approach to fabricate morphable mesostructures with magnetic particles is through the additive manufacture of elastomer composite containing magnetic particles. After dispersing magnetic particles in composite ink, a magnetic field is applied to the microfluidic channel[94] (for digital light projection) or dispensing nozzle[95] (for direct ink writing), enabling reorientation of particles along the magnetic field to impart patterned magnetic polarity to printed filaments. Using this approach, diverse 2D and 3D morphable mesostructures can be encoded with intricate patterns of magnetic domains. Fig. 4(b) shows ferromagnetic soft continuum robots with hydrogel skins[96], in which the tip of the robot is programmed with magnetic polarities, and the hydrogel skin provided a hydrated, self-lubricating layer on the robot's surface. The silica shell coated around the embedded magnetic particles prevented their corrosion at the hydrated interface. This biocompatible soft robot can be omnidirectionally steered- and navigated through the magnetic actuation, and can smoothly navigate through 3D cerebrovascular phantom network without any noticeable difficulties or unintended motion.

Fabrication of morphable mesostructures with individual magnets is relatively simple, as compared to those with magnetic particles. By embedding two permanent magnets to a scallop-like polydimethylsiloxane (PDMS) structure with glue, a single-hinge submillimeter-size swimmer can be achieved, which is capable of propelling in fluids by reciprocal motion, when actuated by an rotating magnetic field[97]. In another example, assisted by two internal magnets, a multi-hinge soft capsule can reversibly change between a cylindrical shape and a stable sphere shape, when subject to a strong magnetic field, showing potential applications in drug delivery[98, 99].

6. Methods and applications of electrically actuated reconfiguration

Electrically responsive morphable mesostructures typically utilized dielectric elastomers (DEs)[100], ionic polymer-metal composites (IPMCs)[101] and piezoelectric/ferroelectric materials[102] to achieve shape reconfigurations. Similar to the magnetic field, the electric field induced actuation can also be controlled accurately and rapidly. Based on this approach, the response time varies from several milliseconds[103, 104] to several seconds[105, 106].

DEs can produce a large actuation strain when two opposite sides are attached to electrodes with different potentials. Coulomb forces drive electrodes closer to each other, and cause an in-plane expansion. When dispersing percolating network of metallic nanowires over the surface of DE, the flat surface can be reversibly and deterministically deformed into non-uniform wavy shapes[107] by electric actuation. DEs can also be used for the fabrication of versatile gripper[108, 109] or electronic fish[110]. As shown in the left-hand panel of Fig. 5(a), a thin hydrogel electrode is sandwiched between two biaxially prestretched DE membranes, and two liquid silicone precursors are attached on the top of DE membrane to form the soft body. Without applying any voltage, the body maintains a bent state at equilibrium. When a voltage is applied, the DE membrane expands and the curvature of soft body is reduced. When a periodic voltage is applied, the fins in the body flap and the electronic fish can swim at a speed as high as 13.5 cm/s (right-hand panel in Fig. 5(a)).

IPMC is composed of ion-conducting polymer with electrodes on both sides. Upon hydration, the positive ions in the polymer can move freely, whereas the negative ions are bonded with carbon chains in the polymer. When a voltage is applied to the electrodes, the positively charged ions move to the cathode, and a bending effect occurs due to the uneven distribution of molecules[111]. The top panel of Fig. 5(b) shows four IPMC actuators move back and forth in sequence, when different voltages are applied. This can be used as a type of

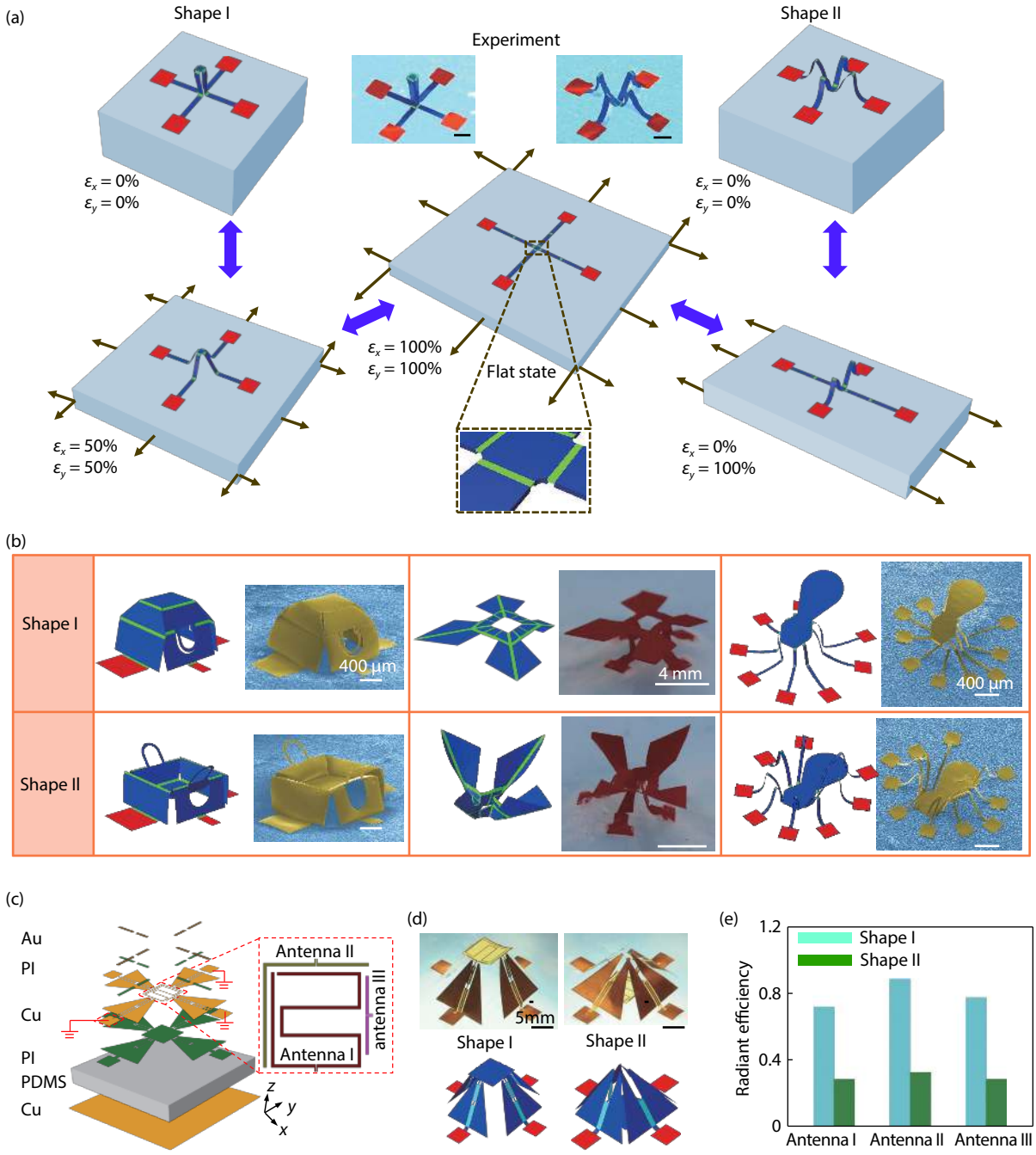

Fig. 6. (Color online) Methods and applications of mechanically actuated reconfiguration through the use of different strain release paths. (a) Illustration of the strategy through a sequence of FEA results and a pair of colorized SEM images for the two stable configurations. (b) SEM images and FEA predictions of morphable, recognizable objects. (c) Exploded view of the layer construction for a morphable electromagnetic device with shielding capability. (d) Optical images and FEA predictions of the device. (e) Simulated radiant efficiency of three antennas at two different stable shapes. Reproduced with permission from Ref. [137]. Copyright 2018, Macmillan Publishers Limited.

gripper. As shown in the bottom panel of Fig. 5(b), upon the application of a 3 V voltage, the three-finger gripper can pick up an object weighing 0.07 g[101]. Other applications of IPMC include underwater vehicles[112], catheter robots[113] and self-rolling wheels[114].

Due to their stable thermal and chemical properties[115] and high power density (scales as L^{-1}, where L is the length of the actuator)[116], piezoelectric materials have been regarded as one of the most widely used electrically actuated materials. Light-weighted soft robots made of piezoelectric materials can achieve good mobility and robustness[117]. Fig. 5(c) shows the movement of an insect-scale robot[118–120]. The robot consists of a curved body and a leg-like structure at the front, made of multilayers including poly(vinylidene fluoride) (PVDF), palladium (Pd)/gold (Au) electrodes, adhesive silicone, and polyethylene terephthalate (PET) substrate. The PVDF layer can produce periodic extension and contraction by the piezoelectric effect under an AC driving voltage to change the shape of the body, leading to the locomotion of the robot. In another example, microscale aerial vehicle assisted by piezoelectric actuators can achieve sustained untethered flight, whose weight and energy consume are as

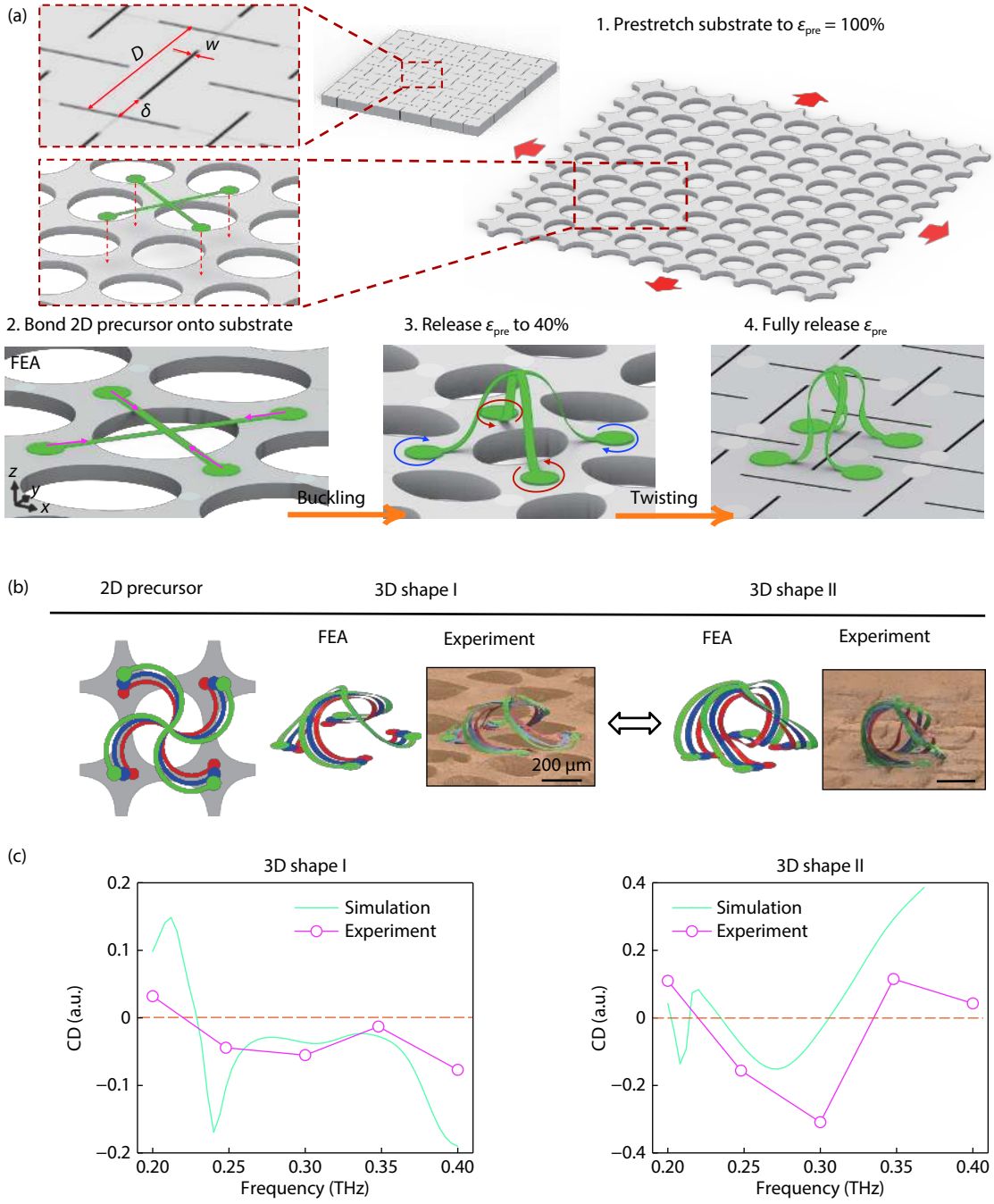

Fig. 7. (Color online) Methods and applications of mechanically actuated reconfiguration assisted by kirigami substrate designs. (a) Conceptual illustration of the fabrication process, through a sequence of FEA results. (b) Two-dimensional geometries, FEA predictions, and scanning electron microscope images of a 3D morphable trilayer microstructure as mechanically tunable optical chiral metamaterials. (c) Measured and simulated optical circular dichroism of the 3D trilayer microstructure with two 3D shapes in the 0.2–0.4-THz frequency range. Reproduced with permission from Ref. [5], Copyright 2019, National Academy of Sciences.

little as 259 mg and 120 mW, respectively[121].

7. Methods and applications of mechanically actuated reconfiguration

Mechanically actuated reconfiguration approaches are developed based on the buckling-guided assembly that exploits prestrained elastomer platform to provide mechanical forces to drive the 3D assembly[122–127]. These reconfiguration methods are compatible with nearly any class of thin film materials[128, 129], including those used in state-of-the-art semiconductor industries[130–132]. The process occurs in a parallel fashion at high throughput, over length scales from submicron to several centimeters[133–136].

This type of reconfiguration approach relies on different strain release paths of substrates to reshape the spatial geometries[137, 138]. Fig. 6(a) presents the scheme for reconfiguration process. Application of an equal 100% biaxial strain drives the assembled column structure (Shape I) to a flat 2D cross-ribbon film. Sequential release of the biaxial strain reshapes the 2D structure further into a socket structure (Shape II). Fig. 6(b) illustrates three examples of reconfigurable mesostructures, including those that can be reshaped between a

Table 1. Summary of reconfiguration methods.

Stimuli type	Mechanism/material	Advantage	Disadvantage	Response time	Reference
Thermal stimuli	Shape-memory polymers	Remote actuation; Large actuation strain	Slow response Low actuation force	15 min	[32]
	Thermally responsive hydrogel	Low transition temperature	Relatively slow response	5–10 s	[37]
	Liquid crystal elastomers	Remote actuation; Complex reconfigurable geometry	Relatively slow response	15 s	[22, 23]
	Shape-memory alloys	High energy density; Large actuation strain and force	Limited operating temperature; Low bandwidth	0.15–14 s	[18, 140]
	Transition metal oxides	Remote actuation; High work density; Fast response	Low bandwidth	0.34–12.5 ms	[19, 141]
Chemical stimuli	Swelling deformation/ hydrogel	Fast response possible biocompatible	Sensitive to environment	0.4 s –1 min	[51, 60, 63]
	Swelling deformation/ inorganic materials	Large actuation force	Sensitive to environment	3.4 s	[65]
	Change of swelling ratio	Biocompatible	Slow response; Sensitive to environment	10 min	[52]
Optical stimuli	Direct activation	Remote actuation; Fast response	Low thermal stability	12.5 ms	[73, 75, 142]
	Indirect activation	Remote actuation	Relatively slow response	30 s	[67]
Magnetic stimuli	Conventional polymer fabrication with magnetic particles	Remote actuation; Fast response; Multiple reconfigurable geometry	Low actuation force for microscale structures	<0.25 s	[88]
	Additive manufacture with magnetic particles	Remote actuation; Fast response complex initial geometry	Low actuation force for microscale structures	<0.5 s	[95]
	Individual magnets	Remote actuation; Fast response	Challenging to scale down to microscale	0.4 s	[98, 99, 143]
Electric stimuli	Dielectric elastomers	Large actuation strain; Fast response	High voltage	<1 ms	[144]
	Ionic polymer-metal composites	Low voltage	Relatively slow response	14 s	[105]
	Piezoelectric materials	Stable thermal and chemical properties; High power density; Fast response	Relatively high voltage	<5 ms	[121]
Mechanical stimuli	Strain release paths of substrates	Parallel reconfiguration; Diverse compatible material; Large applicable length scale; Multiple and complex reconfigurable geometry	Relatively slow response	>20 s	[137, 139]

'house' and a 'shopping bag', or between a 'maple leaf' and a 'bird', or between an 'octopus' and a 'spider'. With appropriated designs of 2D precursors, mesostructures with unique buckling mode can be also stabilized at a relative high buckling mode, by harnessing the interface adhesion of the film/substrate system[139]. Figs. 6(c)–6(e) shows a concealable electromagnetic device that consists of two key parts, an electromagnetically shielding structure and three antennas on the middle pad (Fig. 6(c)). The simultaneous release yields a configuration corresponding to the working mode (Shape I, Fig. 6(d)), where the antennas are elevated and exposed. The sequential release leads to a reshaped system in the concealing mode (Shape II, Fig. 6(d)) where the metallic shielding structure covers the coil. The simulation results showed that the Shape II has a much smaller radiant efficiency than Shape I for all three antennas, as shown in Fig. 6(e).

Engineered kirigami cuts of the substrate were developed to facilitate the reconfiguration of the mesostructures[5], by introducing evident twisting deformations. Fig. 7(a) presents a schematic illustration for forming 3D mesostructures on kirigami substrates. The elastomeric assembly substrates are deformed into interconnected segments that rotate relative to one another during stretching. Release of the substrate involves a 2-stage process that first drives the transformation of a 2D precursor into an initial 3D structure by conventional buckling and then introduces strong and well-defined levels of rotational twist to yield the final shape. Figs. 7(b) and 7(c) shows a mechanically tunable optical chiral metamaterial consisting of a trilayer of mutually twisted or conjugated rosettes. Controlled release of the substrate provides access to two morphable 3D shapes, as shown in Fig. 7(b). The distinct microscale geometries of these two shapes give rise to mutually detuned resonant responses in the terahertz (THz) range. Experimental measurements of the helical microstructure under left-handed and right-handed circularly polarized light (LCP and RCP) exhibit wavelength-dependent chirality, or asymmetric absorption, in the 0.2–0.4 THz range.

8. Summary and outlook

This paper offered a detailed overview of reconfiguration methodologies of 3D mesostructures with feature sizes that range from submicrons to centimeters. The reconfiguration can be achieved by thermal, chemical, optical, electric, magnetic, or mechanical means, through use of diverse materials such as soft polymers, metals, and their heterogeneous combinations, as summarized in Table 1.

Although remarkable progress has been made in the area of 3D reconfiguration approaches, many challenges remain and fruitful opportunities exist for future exploration.

Some of these approaches need a long actuation time to trigger reconfiguration, such as the thermal actuation (response time around 1–10 s, except for VO_2-based actuation), the indirect light actuation (~30 s), and the chemical actuation (more than 1 min for some hydrogels swelling). Besides, morphable mesostructures activated directly by light are usually in low thermal stabilities because the cis-azobenzene tends to destabilize the phase structures of the LCE mixture, resulting in a failure of shape reconfiguration. The magnetic reconfiguration methods can only generate a low actuation force that scales with the structure volume (L^3) and decreases exponentially as L shrinks. This feature limits their applications at microscale. Electrically responsive materials such as DEs require high driving voltages on the order of kV, which are often close to the electrical breakdown voltage of materials. Mechanically actuated reconfiguration methods involve a complex transformation process that depends not only on the layouts of 2D precursor but also on the substrate designs and loading strategy. Together with the non-linearity of bifurcation induced by buckling, the inverse design to achieve two desired stable configurations is very challenging. Except for the mechanical reconfiguration method, almost all of the other reconfiguration methods are not compatible with state-of-the-art semiconductor technologies, and their deformations are mainly limited to bending/folding, contraction, and expansion. Finally, compared with multi-functional devices depending on other reconfiguration methods, such as switching components or smart materials (sensitive in electric permittivity or magnetic permeability), the morphable devices based on physical reconfiguration methods may have a lower degree of integration, which means that only limited functions can be achieved by reconfiguration.

In addition to solving the challenges of reconfiguration approaches mentioned above, some other research directions are also essential for the development of reconfiguration technology. One significant segment of research interest for morphable mesostructures is related to the biomedical applications for in-body diagnosis and treatment. Consequently, it is desirable to develop more biocompatible active materials that can operate upon safe stimuli condition. Moreover, deformation control principles that predict the correlation between geometric configuration and the property of stimuli play an important role in the inverse design and practical applications.

References

[1] Hines L, Petersen K, Lum G Z, et al. Soft actuators for small-scale robotics. Adv Mater, 2017, 29(13), 1603483

[2] Kotikian A, McMahan C, Davidson E C, et al. Untethered soft robotic matter with passive control of shape morphing and propulsion. Sci Robot, 2019, 4(33), eaax7044

[3] Anderson I A, Gisby T A, McKay T G, et al. Multi-functional dielectric elastomer artificial muscles for soft and smart machines. J Appl Phys, 2012, 112(4), 041101

[4] Cheng X, Zhang Y. Micro/nanoscale 3D assembly by rolling, folding, curving, and buckling approaches. Adv Mater, 2019, 31, 1901895

[5] Zhao H, Li K, Han M, et al. Buckling and twisting of advanced materials into morphable 3D mesostructures. Proc Natl Academ Sci United States Am, 2019, 116(27), 13239

[6] Lum G Z, Ye Z, Dong X, et al. Shape-programmable magnetic soft matter. Proceedings of the National Academy of Sciences of the United States of America, 2016, 113(41), E6007

[7] Lendlein A, Gould O E C. Reprogrammable recovery and actuation behaviour of shape-memory polymers. Nat Rev Mater, 2019, 4(2), 116

[8] Liu Y, Genzer J, Dickey M D. "2D or not 2D": Shape-programming polymer sheets. Prog Polym Sci, 2016, 52, 79

[9] Xu B, Zhang B, Wang L, et al. Tubular micro/nanomachines: from the basics to recent advances. Adv Funct Mater, 2018, 28(25), 1705872

[10] Li J, Liu T, Xia S, et al. A versatile approach to achieve quintuple-shape memory effect by semi-interpenetrating polymer networks containing broadened glass transition and crystalline segments. J Mater Chem, 2011, 21(33), 12213

[11] Hager M D, Bode S, Weber C, et al. Shape memory polymers: past, present and future developments. Prog Polym Sci, 2015, 49/50, 3

[12] Xie T. Tunable polymer multi-shape memory effect. Nature, 2010, 464(7286), 267

[13] Behl M, Kratz K, Noechel U, et al. Temperature-memory polymer actuators. Proceedings of the National Academy of Sciences of the United States of America, 2013, 110(31), 12555

[14] Wang Y, Villada A, Zhai Y, et al. Tunable surface wrinkling on shape memory polymers with application in smart micromirror. Appl Phys Lett, 2019, 114(19), 193701

[15] Wang Y, Zhai Y, Villada A, et al. Programmable localized wrinkling of thin films on shape memory polymers with application in nonuniform optical gratings. Appl Phys Lett, 2018, 112(25), 251603

[16] Noh M, Kim S W, An S, et al. Flea-inspired catapult mechanism for miniature jumping robots. IEEE Trans Robot, 2012, 28(5), 1007

[17] Fu Y Q, Du H J, Huang W M, et al. TiNi-based thin films in MEMS applications: a review. Sens Actuators A, 2004, 112(2/3), 395

[18] Fu Y Q, Luo J K, Flewitt A J, et al. Microactuators of free-standing TiNiCu films. Smart Mater Struct, 2007, 16(6), 2651

[19] Liu K, Cheng C, Suh J, et al. Powerful, multifunctional torsional micromuscles activated by phase transition. Adv Mater, 2014, 26(11), 1746

[20] Wang T, Torres D, Fernandez F E, et al. Maximizing the performance of photothermal actuators by combining smart materials with supplementary advantages. Sci Adv, 2017, 3(4), e1602697

[21] Rúa A, Fernández F E, Sepúlveda N. Bending in VO_2-coated microcantilevers suitable for thermally activated actuators. J Appl Phys, 2010, 107(7), 074506

[22] Ware T H, McConney M E, Wie J J, et al. Voxelated liquid crystal elastomers. Science, 2015, 347(6225), 982

[23] de Haan L T, Gimenez-Pinto V, Konya A, et al. Accordion-like actuators of multiple 3D patterned liquid crystal polymer films. Adv Funct Mater, 2014, 24(9), 1251

[24] Yang Y, Pei Z, Li Z, et al. Making and remaking dynamic 3D structures by shining light on flat liquid crystalline vitrimer films without a mold. J Am Chem Soc, 2016, 138(7), 2118

[25] Ahn C, Liang X, Cai S. Inhomogeneous stretch induced patterning of molecular orientation in liquid crystal elastomers. Extrem Mechan Lett, 2015, 5, 30

[26] Pei Z, Yang Y, Chen Q, et al. Mouldable liquid-crystalline elastomer actuators with exchangeable covalent bonds. Nat Mater, 2014, 13(1), 36

[27] Bormashenko E, Bormashenko Y, Pogreb R, et al. Janus droplets: liquid marbles coated with dielectric/semiconductor particles. Langmuir, 2011, 27(1), 7

[28] Lemanowicz M, Gierczycki A, Kuznik W, et al. Determination of lower critical solution temperature of thermosensitive flocculants. Miner Eng, 2014, 69, 170

[29] Stoychev G, Turcaud S, Dunlop J W C, et al. Hierarchical multi-

step folding of polymer bilayers. Adv Funct Mater, 2013, 23(18), 2295
[30] Stroganov V, Al-Hussein M, Sommer J U, et al. Reversible thermosensitive biodegradable polymeric actuators based on confined crystallization. Nano Lett, 2015, 15(3), 1786
[31] Wang E, Desai M S, Lee S W. Light-controlled graphene-elastin composite hydrogel actuators. Nano Lett, 2013, 13(6), 2826
[32] Jin B, Song H, Jiang R, et al. Programming a crystalline shape memory polymer network with thermo- and photo-reversible bonds toward a single-component soft robot. Sci Adv, 2018, 4(1), eaao3865
[33] Wall S, Wegkamp D, Foglia L, et al. Ultrafast changes in lattice symmetry probed by coherent phonons. Nat Commun, 2012, 3, 721
[34] Cao J, Ertekin E, Srinivasan V, et al. Strain engineering and one-dimensional organization of metal-insulator domains in single-crystal vanadium dioxide beams. Nat Nanotechnol, 2009, 4(11), 732
[35] Fusco S, Sakar M S, Kennedy S, et al. An integrated microrobotic platform for on-demand, targeted therapeutic interventions. Adv Mater, 2014, 26(6), 952
[36] Miyashita S, Meeker L, Tolley M T, et al. Self-folding miniature elastic electric devices. Smart Mater Struct, 2014, 23(9), 094005
[37] Stoychev G, Puretskiy N, Ionov L. Self-folding all-polymer thermoresponsive microcapsules. Soft Matter, 2011, 7(7), 3277
[38] Yoon C, Xiao R, Park J, et al. Functional stimuli responsive hydrogel devices by self-folding. Smart Mater Struct, 2014, 23(9), 094008
[39] Verduzco R. Shape-shifting liquid crystals. Science, 2015, 347(6225), 949
[40] Palagi S, Mark A G, Reigh S Y, et al. Structured light enables biomimetic swimming and versatile locomotion of photoresponsive soft microrobots. Nat Mater, 2016, 15(6), 647
[41] Cui Y, Wang C, Sim K, et al. A simple analytical thermo-mechanical model for liquid crystal elastomer bilayer structures. AIP Adv, 2018, 8(2), 025215
[42] Wang C, Sim K, Chen J, et al. Soft ultrathin electronics innervated adaptive fully soft robots. Adv Mater, 2018, 30(13), 1706695
[43] He Q, Wang Z, Wang Y, et al. Electrically controlled liquid crystal elastomer-based soft tubular actuator with multimodal actuation. Sci Adv, 2019, 5(10), eaax5746
[44] Kim S, Hawkes E, Cho K, et al. Micro artificial muscle fiber using NiTi spring for soft robotics. 2009 IEEE/RSJ International Conference on Intelligent Robots and Systems, 2009, 2228
[45] Ali M S M, Takahata K. Frequency-controlled wireless shape-memory-alloy microactuators integrated using an electroplating bonding process. Sens Actuators A, 2010, 163(1), 363
[46] Colorado J, Barrientos A, Rossi C, et al. Biomechanics of smart wings in a bat robot: morphing wings using SMA actuators. Bioinspir Biomimet, 2012, 7(3), 036006
[47] Furst S J, Bunget G, Seelecke S. Design and fabrication of a bat-inspired flapping-flight platform using shape memory alloy muscles and joints. Smart Mater Struct, 2012, 22(1), 014011
[48] Liu K, Cheng C, Cheng Z, et al. Giant-amplitude, high-work density microactuators with phase transition activated nanolayer bimorphs. Nano Lett, 2012, 12(12), 6302
[49] Wang K, Cheng C, Cardona E, et al. Performance limits of microactuation with vanadium dioxide as a solid engine. ACS Nano, 2013, 7(3), 2266
[50] Tian Z, Huang W, Xu B, et al. Anisotropic rolling and controlled chirality of nanocrystalline diamond nanomembranes toward biomimetic helical frameworks. Nano Lett, 2018, 18(6), 3688
[51] Zhao Q, Dunlop J W C, Qiu X, et al. An instant multi-responsive porous polymer actuator driven by solvent molecule sorption. Nat Commun, 2014, 5, 4293
[52] Xiao R, Guo J, Safranski D L, et al. Solvent-driven temperature memory and multiple shape memory effects. Soft Matter, 2015, 11(20), 3977
[53] Huang W M, Yang B, An L, et al. Water-driven programmable polyurethane shape memory polymer: Demonstration and mechanism. Appl Phys Lett, 2005, 86(11), 114105
[54] Ma M, Guo L, Anderson D G, et al. Bio-inspired polymer composite actuator and generator driven by water gradients. Science, 2013, 339(6116), 186
[55] Chen X, Goodnight D, Gao Z, et al. Scaling up nanoscale water-driven energy conversion into evaporation-driven engines and generators. Nat Commun, 2015, 6, 7346
[56] Lee B P, Konst S. Novel hydrogel actuator inspired by reversible mussel adhesive protein chemistry. Adv Mater, 2014, 26(21), 3415
[57] Jamal M, Zarafshar A M, Gracias D H. Differentially photo-crosslinked polymers enable self-assembling microfluidics. Nat Commun, 2011, 2, 527
[58] Kim J, Hanna J A, Byun M, et al. Designing responsive buckled surfaces by halftone gel lithography. Science, 2012, 335(6073), 1201
[59] Gladman A S, Matsumoto E A, Nuzzo R G, et al. Biomimetic 4D printing. Nat Mater, 2016, 15(4), 413
[60] Palleau E, Morales D, Dickey M D, et al. Reversible patterning and actuation of hydrogels by electrically assisted ionoprinting. Nat Commun, 2013, 4, 2257
[61] Lee H, Xia C, Fang N X. First jump of microgel; actuation speed enhancement by elastic instability. Soft Matter, 2010, 6(18), 4342
[62] Zhang H, Guo X, Wu J, et al. Soft mechanical metamaterials with unusual swelling behavior and tunable stress-strain curves. Sci Adv, 2018, 4(6), eaar8535
[63] Ollagnier A, Fabre A, Thundat T, et al. Activation process of reversible Pd thin film hydrogen sensors. Sens Actuators B, 2013, 186, 258
[64] Xu B, Zhang X, Tian Z, et al. Microdroplet-guided intercalation and deterministic delamination towards intelligent rolling origami. Nat Commun, 2019, 10(1), 5019
[65] Xu B, Tian Z, Wang J, et al. Stimuli-responsive and on-chip nanomembrane micro-rolls for enhanced macroscopic visual hydrogen detection. Sci Adv, 2018, 4(4), eaap8203
[66] Gestos A, Whitten P G, Wallace G G, et al. Actuating individual electrospun hydrogel nanofibres. Soft Matter, 2012, 8(31), 8082
[67] Techawanitchai P, Ebara M, Idota N, et al. Photo-switchable control of pH-responsive actuators via pH jump reaction. Soft Matter, 2012, 8(10), 2844
[68] Ma C, Li T, Zhao Q, et al. Supramolecular Lego assembly towards three-dimensional multi-responsive hydrogels. Adv Mater, 2014, 26(32), 5665
[69] Dong L, Agarwal A K, Beebe D J, et al. Adaptive liquid microlenses activated by stimuli-responsive hydrogels. Nature, 2006, 442(7102), 551
[70] Yu Y, Ikeda T. Soft actuators based on liquid-crystalline elastomers. Angew Chem Int Ed, 2006, 45(33), 5416
[71] Yu M F, Files B S, Arepalli S, et al. Tensile loading of ropes of single wall carbon nanotubes and their mechanical properties. Phys Rev Lett, 2000, 84(24), 5552
[72] Wei J, Yu Y. Photodeformable polymer gels and crosslinked liquid-crystalline polymers. Soft Matter, 2012, 8(31), 8050
[73] White T J, Tabiryan N V, Serak S V, et al. A high frequency photodriven polymer oscillator. Soft Matter, 2008, 4(9), 1796
[74] Zeng H, Wasylczyk P, Parmeggiani C, et al. Light-fueled microscopic walkers. Adv Mater, 2015, 27(26), 3883
[75] Tang X, Tang S Y, Sivan V, et al. Photochemically induced motion of liquid metal marbles. Appl Phys Lett, 2013, 103(17), 174104
[76] Lendlein A, Jiang H Y, Junger O, et al. Light-induced shape-memory polymers. Nature, 2005, 434(7035), 879

[77] Jiang H Y, Kelch S, Lendlein A. Polymers move in response to light. Adv Mater, 2006, 18(11), 1471
[78] Yu Y L, Nakano M, Ikeda T. Directed bending of a polymer film by light . Nature, 2003, 425(6954), 145
[79] Natansohn A, Rochon P. Photoinduced motions in azo-containing polymers. Chem Rev, 2002, 102(11), 4139
[80] Lee K M, Koerner H, Vaia R A, et al. Light-activated shape memory of glassy, azobenzene liquid crystalline polymer networks. Soft Matter, 2011, 7(9), 4318
[81] Huang C, Lv J A, Tian X, et al. Miniaturized swimming soft robot with complex movement actuated and controlled by remote light signals. Sci Rep, 2015, 5, 17414
[82] Yamada M, Kondo M, Mamiya J, et al. Photomobile polymer materials: towards light-driven plastic motors. Angew Chem, 2008, 47(27), 4986
[83] Boncheva M, Andreev S A, Mahadevan L, et al. Magnetic self-assembly of three-dimensional surfaces from planar sheets. Proc Natl Academ Sci United States of Am, 2005, 102(11), 3924
[84] Solovev A A, Sanchez S, Pumera M, et al. Nanomotors: magnetic control of tubular catalytic microbots for the transport, assembly, and delivery of micro-objects. Adv Funct Mater, 2010, 20(15), 2430
[85] Fusco S, Huang H W, Peyer K E, et al. Shape-switching microrobots for medical applications: the influence of shape in drug delivery and locomotion. Acs Appl Mater Interfaces, 2015, 7(12), 6803
[86] Tasoglu S, Diller E, Guven S, et al. Untethered micro-robotic coding of three-dimensional material composition. Nat Commun, 2014, 5, 3124
[87] Diller E, Giltinan J, Lum G Z, et al. Six-degree-of-freedom magnetic actuation for wireless microrobotics. Int J Robot Res, 2016, 35(1–3), 114
[88] Diller E, Zhuang J, Lum G Z, et al. Continuously distributed magnetization profile for millimeter-scale elastomeric undulatory swimming. Appl Phys Lett, 2014, 104(17), 174101
[89] Jang B, Gutman E, Stucki N, et al. Undulatory locomotion of magnetic multilink nanoswimmers. Nano Lett, 2015, 15(7), 4829
[90] Timonen J V I, Latikka M, Leibler L, et al. Switchable static and dynamic self-assembly of magnetic droplets on superhydrophobic surfaces. Science, 2013, 341(6143), 253
[91] Jamin T, Py C, Falcon E. Instability of the origami of a ferrofluid drop in a magnetic field. Phys Rev Lett, 2011, 107(20), 204503
[92] Hu W, Lum G Z, Mastrangeli M, et al. Small-scale soft-bodied robot with multimodal locomotion. Nature, 2018, 554(7690), 81
[93] Garstecki P, Tierno P, Weibel D B, et al. Propulsion of flexible polymer structures in a rotating magnetic field. J Phys Conden Matter, 2009, 21(20), 204110
[94] Kim J, Chung S E, Choi S E, et al. Programming magnetic anisotropy in polymeric microactuators. Nat Mater, 2011, 10(10), 747
[95] Kim Y, Yuk H, Zhao R, et al. Printing ferromagnetic domains for untethered fast-transforming soft materials. Nature, 2018, 558(7709), 274
[96] Kim Y, Parada G A, Liu S, et al. Ferromagnetic soft continuum robots. Sci Robot, 2019, 4(33), eaax7329
[97] Qiu T, Lee T C, Mark A G, et al. Swimming by reciprocal motion at low Reynolds number. Nat Commun, 2014, 5, 5119
[98] Yim S, Sitti M. Design and rolling locomotion of a magnetically actuated soft capsule endoscope. IEEE Trans Robot, 2012, 28(1), 183
[99] Yim S, Sitti M. Shape-programmable soft capsule robots for semi-implantable drug delivery. IEEE Trans Robot, 2012, 28(5), 1198
[100] Brochu P, Pei Q. Advances in dielectric elastomers for actuators and artificial muscles. Macromolecul Rapid Commun, 2010, 31(1), 10
[101] Park I S, Jung K, Kim D, et al. Physical principles of ionic polymer-metal composites as electroactive actuators and sensors. MRS Bull, 2008, 33(3), 190
[102] Miehe C, Rosato D. A rate-dependent incremental variational formulation of ferroelectricity. Int J Eng Sci, 2011, 49(6), 466
[103] Mirfakhrai T, Oh J, Kozlov M, et al. Electrochemical actuation of carbon nanotube yarns. Smart Mater Struct, 2007, 16(2), S243
[104] Foroughi J, Spinks G M, Wallace G G, et al. Torsional carbon nanotube artificial muscles. Science, 2011, 334(6055), 494
[105] Must I, Kaasik F, Põldsalu I, et al. Ionic and capacitive artificial muscle for biomimetic soft robotics. Adv Eng Mater, 2015, 17(1), 84
[106] Palmre V, Pugal D, Kim K J, et al. Nanothorn electrodes for ionic polymer-metal composite artificial muscles. Sci Rep, 2014, 4, 6176
[107] Shian S, Clarke D R. Electrically-tunable surface deformation of a soft elastomer. Soft Matter, 2016, 12(13), 3137
[108] Shintake J, Rosset S, Schubert B, et al. Versatile soft grippers with intrinsic electroadhesion based on multifunctional polymer actuators. Adv Mater, 2016, 28(2), 231
[109] Kofod G, Wirges W, Paajanen M, et al. Energy minimization for self-organized structure formation and actuation. Appl Phys Lett, 2007, 90(8), 081916
[110] Li T, Li G, Liang Y, et al. Fast-moving soft electronic fish. Sci Adv, 2017, 3(4), e1602045
[111] Chu W S, Lee K T, Song S H, et al. Review of biomimetic underwater robots using smart actuators. Int J Prec Eng Manufact, 2012, 13(7), 1281
[112] Aureli M, Kopman V, Porfiri M. Free-locomotion of underwater vehicles actuated by ionic polymer metal composites. IEEE/ASME Trans Mechatron, 2010, 15(4), 603
[113] Barramba J, Silva J, Branco P J C. Evaluation of dielectric gel coating for encapsulation of ionic polymer-metal composite (IPMC) actuators. Sens Actuators A, 2007, 140(2), 232
[114] Must I, Kaasik T, Baranova I, et al. A power-autonomous self-rolling wheel using ionic and capacitive actuators. Proc SPIE, 2015, 9430, 94300Q
[115] Mohammadi B, Yousefi A A, Bellah S M. Effect of tensile strain rate and elongation on crystalline structure and piezoelectric properties of PVDF thin films. Polymer Testing, 2007, 26(1), 42
[116] Smith G L, Pulskamp J S, Sanchez L M, et al. PZT-based piezoelectric MEMS technology. J Am Ceram Soc, 2012, 95(6), 1777
[117] Fuller S B, Karpelson M, Censi A, et al. Controlling free flight of a robotic fly using an onboard vision sensor inspired by insect ocelli. J Royal Soc Interface, 2014, 11(97), 20140281
[118] Wu Y, Yim J K, Liang J, et al. Insect-scale fast moving and ultrarobust soft robot. Sci Robot, 2019, 4(32), eaax1594
[119] Ma K Y, Chirarattananon P, Fuller S B, et al. Controlled flight of a biologically inspired, insect-scale robot. Science, 2013, 340(6132), 603
[120] Chen Y, Doshi N, Goldberg B, et al. Controllable water surface to underwater transition through electrowetting in a hybrid terrestrial-aquatic microrobot. Nat Commun, 2018, 9(1), 2495
[121] Jafferis N T, Helbling E F, Karpelson M, et al. Untethered flight of an insect-sized flapping-wing microscale aerial vehicle. Nature, 2019, 570(7762), 491
[122] Xu S, Yan Z, Jang K I, et al. Assembly of micro/nanomaterials into complex, three-dimensional architectures by compressive buckling. Science, 2015, 347(6218), 154
[123] Zhang Y, Yan Z, Nan K, et al. A mechanically driven form of Kirigami as a route to 3D mesostructures in micro/nanomembranes. Proceedings of the National Academy of Sciences of the United States of America, 2015, 112(38), 11757
[124] Liu Y, Yan Z, Lin Q, et al. Guided formation of 3D helical mesostructures by mechanical buckling: analytical modeling and experimental validation. Adv Funct Mater, 2016, 26(17), 2909
[125] Yan Z, Zhang F, Liu F, et al. Mechanical assembly of complex, 3D

mesostructures from releasable multilayers of advanced materials. Sci Adv, 2016, 2(9), e1601014
[126] Fan Z, Hwang K C, Rogers J A, et al. A double perturbation method of postbuckling analysis in 2D curved beams for assembly of 3D ribbon-shaped structures. J Mechan Phys Solids, 2018, 111, 215
[127] Song J. Mechanics of stretchable electronics. Curr Opin Solid State Mater Sci, 2015, 19(3), 160
[128] Zhang Y, Zhang F, Yan Z, et al. Printing, folding and assembly methods for forming 3D mesostructures in advanced materials. Nat Rev Mater, 2017, 2(4), 17019
[129] Guo X, Xu Z, Zhang F, et al. Reprogrammable 3D mesostructures through compressive buckling of thin films with prestrained shape memory polymer. Acta Mechan Solida Sinica, 2018, 31(5), 589
[130] Jang K I, Li K, Chung H U, et al. Self-assembled three dimensional network designs for soft electronics. Nat Commun, 2017, 8, 15894
[131] Kim B H, Liu F, Yu Y, et al. Mechanically guided post-assembly of 3D electronic systems. Adv Funct Mater, 2018, 28(48), 1803149
[132] Liu F, Chen Y, Song H, et al. High performance, tunable electrically small antennas through mechanically guided 3D assembly. Small, 2019, 15(1), 1804055
[133] Yan Z, Zhang F, Wang J, et al. Controlled mechanical buckling for origami-inspired construction of 3D microstructures in advanced materials. Adv Funct Mater, 2016, 26(16), 2629
[134] Ning X, Wang H, Yu X, et al. 3D tunable, multiscale, and multistable vibrational micro-platforms assembled by compressive buckling. Adv Funct Mater, 2017, 27(14), 1605914
[135] Shi Y, Zhang F, Nan K, et al. Plasticity-induced origami for assembly of three dimensional metallic structures guided by compressive buckling. Extrem Mechan Lett, 2017, 11, 105
[136] Yan Z, Han M, Yang Y, et al. Deterministic assembly of 3D mesostructures in Adv Mater via compressive buckling: A short review of recent progress. Extrem Mechan Lett, 2017, 11, 96
[137] Fu H, Nan K, Bai W, et al. Morphable 3D mesostructures and microelectronic devices by multistable buckling mechanics. Nat Mater, 2018, 17(3), 268
[138] Luo G, Fu H, Cheng X, et al. Mechanics of bistable cross-shaped structures through loading-path controlled 3D assembly. J Mechan Phys Solids, 2019, 129, 261
[139] Liu Y, Wang X, Xu Y, et al. Harnessing the interface mechanics of hard films and soft substrates for 3D assembly by controlled buckling. Proc Natl Academ Sci, 2019, 116(31), 15368
[140] Jani J M, Leary M, Subic A, et al. A review of shape memory alloy research, applications and opportunities. Mater Des, 2014, 56, 1078
[141] Ma H, Hou J, Wang X, et al. Flexible, all-inorganic actuators based on vanadium dioxide and carbon nanotube bimorphs. Nano Lett, 2017, 17(1), 421
[142] Yu H, Ikeda T. Photocontrollable liquid-crystalline actuators. Adv Mater, 2011, 23(19), 2149
[143] Kwok S W, Morin S A, Mosadegh B, et al. Magnetic assembly of soft robots with hard components. Adv Funct Mater, 2014, 24(15), 2180
[144] Pelrine R, Kornbluh R, Pei Q, et al. High-speed electrically actuated elastomers with strain greater than 100%. Science, 2000, 287(5454), 836